Constraining dark matter capture and annihilation cross sections by searching for neutrino signature from the Earth's core

Fei-Fan Lee,[1] Guey-Lin Lin,[1] and Yue-Lin Sming Tsai[2]

[1]*Institute of Physics, National Chiao-Tung University, Hsinchu 30010, Taiwan*
[2]*National Centre for Nuclear Research, Hoża 69, 00-681 Warsaw, Poland*

(Received 16 August 2013; published 6 January 2014)

We study the sensitivity of IceCube/DeepCore detector to dark matter annihilations in the Earth's core. We focus on annihilation modes $\chi\chi \to \nu\bar{\nu}$, $\tau^+\tau^-$, $b\bar{b}$, and W^+W^-. Both track and cascade events are considered in our analysis. By fixing the dark matter annihilation cross section $\langle\sigma v\rangle$ at some nominal values, we study the sensitivity of the IceCube/DeepCore detector to dark matter spin-independent cross section $\sigma_p^{\rm SI}$ for m_χ ranging from few tens of GeV to 10 TeV. This sensitivity is compared with the existing IceCube 79-string constraint on the same cross section, which was obtained by searching for dark matter annihilations in the Sun. We compare this sensitivity to dark matter direct detection results as well, in particular the XENON100 (2012) limit and the parameter regions preferred by DAMA and CRESST-II experiments. We also present IceCube/DeepCore sensitivity to $\langle\sigma v\rangle$ as a function of m_χ by fixing $\sigma_p^{\rm SI}$ at XENON100 (2012) and XENON1T limits, respectively. This sensitivity is compared with the preferred dark matter parameter range derived from the combined fitting to PAMELA and AMS02 positron fraction data. We conclude that the search for dark matter annihilations in the Earth's core provides competitive constraints on $\sigma_p^{\rm SI}$ and $\langle\sigma v\rangle$ in the case of low-mass dark matter. Particularly, the expected constraint on $\sigma_p^{\rm SI}$ for 5 years of data taking in IceCube/DeepCore is more stringent than the current IceCube 79-string limit mentioned above.

DOI: 10.1103/PhysRevD.89.025003 PACS numbers: 14.60.Pq, 14.60.St

I. INTRODUCTION

Evidence for the dark matter (DM) are provided by many astrophysical observations, although the nature of DM is yet to be uncovered. The most popular candidates for DM are weak interacting massive particles (WIMPs), which we shall assume in this work. Dark matter can be detected either directly or indirectly with the former observing the nucleus recoil as DM interacts with the target nuclei in the detector and the latter detecting final state particles resulting from DM annihilations or decays. The direct detection is possible because the dark matter particles constantly bombard the Earth as the Earth sweeps through the local halos. As just stated, the direct detection experiments record the nuclei recoil energy of nuclei-WIMPs scattering. At present, DAMA [1], CoGeNT [2], and CRESST [3] have reported the detection of DM signal with the DM mass m_χ ranging from few GeV to 50 GeV and the spin-independent scattering cross section $\sigma_p^{\rm SI} \sim 10^{-4}$ pb. On the other hand, XENON100 [4] only collects 2 events which are consistent with the background. This result then sets the limit $\sigma_p^{\rm SI} < 2 \times 10^{-9}$ pb for $m_\chi = 55$ GeV. Interestingly, a recent CDMS II result [5] reports three signal events which gives a p-value 0.19% (less than 4σ). The corresponding best-fit values of DM parameters are $m_\chi = 8.6$ GeV and $\sigma_p^{\rm SI} \sim 1.9 \times 10^{-5}$ pb.

Dark matter can also be detected indirectly by measuring the positron signals from the Milky Way. PAMELA observed a rise of the cosmic ray positron fraction for positron energy greater than 10 GeV [6]. This anomalous enhancement is confirmed by Fermi-LAT [7] and the recently released AMS02 first result [8]. In the recent AMS02 result, this continuous rise of the positron fraction is extended up to positron energy ~350 GeV. Such a spectral behavior makes the DM annihilation explanation of the data difficult because it requires a large boost factor for annihilation cross section $\langle\sigma v\rangle$ provided the thermal equilibrium for DM in the early universe is reached with $\langle\sigma v\rangle \sim 3 \times 10^{-26}$ cm^3 s^{-1}. For example, several groups [9–15] fit the updated galactic positron fraction with the AMS02 new results included. They have found that the favored DM parameter region is located at $m_\chi \sim$ few TeV and $10^{-23} \lesssim \langle\sigma v\rangle/{\rm cm}^3\,{\rm s}^{-1} \lesssim 10^{-21}$ if DM annihilation channel $\chi\chi \to \tau^+\tau^-$ is responsible for the positron excess. The favored DM mass range can be lowered to a few hundred GeV if nearby pulsar sources are considered together with $\chi\chi \to \tau^+\tau^-$ annihilations [12]. However, the favored values for $\langle\sigma v\rangle$ do not decrease much in such a combined fitting. It is important to note that DM annihilations in the galactic halo are constrained by Fermi-LAT gamma ray observations [16]. The constraint on $\langle\sigma(\chi\chi \to \tau^+\tau^-)v\rangle$ is in fact located in the preferred DM parameter region resulting from PAMELA and AMS02 measurements for the same range of m_χ.

It has been pointed out some time ago that the preferred DM parameter region by PAMELA and Fermi-LAT measurements can be examined through the observation of neutrinos [17–19] (see also discussions in Refs. [20,21]) by the

IceCube detector augmented with DeepCore array. Indeed IceCube 22 string result on searching for DM annihilations from the galactic halo [22] has set the upper limit for $\langle\sigma(\chi\chi \to \tau^+\tau^-)v\rangle$ comparable to the required annihilation cross section for explaining PAMELA and Fermi-LAT data. The IceCube sensitivity on DM signature from the galactic halo is expected to improve with the data from all 86 strings analyzed. The analysis of DeepCore array data will further enhance the sensitivity in the small m_χ regime [23,24] which is of interest due to direct detection results mentioned above.

It is interesting to note that the constraints on DM capture cross section and annihilation cross section $\langle\sigma v\rangle$ can be obtained from the searching for DM annihilations from the Earth's core. The detection of DM-induced neutrino signature from the Earth's core has been discussed previously [25–28]. It has been shown that the chemical composition of the Earth's core results in several DM annihilation peaks for m_χ ranging from 20 to 60 GeV. These peaks do not appear for annihilations inside the Sun. Furthermore, the DM annihilation rate inside the Sun is completely determined by the capture cross section (contributed by both spin-dependent cross section $\sigma_p^{\rm SD}$ and spin-independent cross section $\sigma_p^{\rm SI}$, respectively) while DM annihilation rate in the Earth's core depends on both $\sigma_p^{\rm SI}$ (contribution proportional to $\sigma_p^{\rm SD}$ is negligible) and $\langle\sigma v\rangle$. This is understood by the fact that DM density in the former case has already reached equilibrium while DM density in the latter case has not. Hence the search for neutrino signature from the Earth's core can probe both cross sections.

Model-independent sensitivity studies on IceCube detection of DM induced neutrino signature from the Earth core were reported in [29,30] for DM mass around TeV. In this work, we consider an extended DM mass range from a few tens of GeV to TeV. In the low mass range, our results can be compared with direct detection results from DAMA, CoGeNT, CRESST-II, and XENON100 mentioned above. In the high mass range around TeV, our results can be compared with those from cosmic ray observations by PAMELA, Fermi-LAT, and AMS02. We study both muon track events and cascade events induced by neutrinos. We consider annihilation channels $\chi\chi \to \nu\bar{\nu}$, $\chi\chi \to \tau^+\tau^-$, W^+W^-, $b\bar{b}$ for signature neutrino productions. For nonmonochromatic modes, we note that $\chi\chi \to \tau^+\tau^-$ produces the hardest neutrino spectrum while $\chi\chi \to b\bar{b}$ produces the softest one. We also include $\nu_\mu \to \nu_\tau$ oscillations for lower energy neutrinos.

This paper is organized as follows. In Sec. II, we discuss the neutrino flux produced in the Earth's core by DM annihilations. The procedure for calculating such a flux is outlined. In Sec. III, we discuss the track and shower event rates resulting from DM annihilations in the Earth's core. The background event rates from atmospheric neutrino flux are also calculated. We adopt the effective areas published by the IceCube observatory for event rate calculations. In Sec. IV, we present IceCube/DeepCore 5-year sensitivities for detecting DM-induced neutrino signature from the Earth's core. We first fix the DM mass at two representative values, $m_\chi = 50$ GeV and $m_\chi = 2$ TeV. The IceCube/DeepCore 2σ sensitivity for 5-year data taking is then presented as a curve on $(\langle\sigma v\rangle, \sigma_p^{\rm SI})$ plane. Next, we fix the annihilation cross section $\langle\sigma v\rangle$ at conservative values, 3×10^{-26} cm^3 s^{-1} and 3×10^{-27} cm^3 s^{-1}. We then present IceCube/DeepCore sensitivities to spin-independent cross section $\sigma_p^{\rm SI}$ as a function of m_χ for different assumptions on dominant DM annihilation channels. Such sensitivities are then compared with existing constraints from direct detection experiments and that obtained from the IceCube/DeepCore search of DM annihilations in the Sun. Finally, we take different experimental bounds on $\sigma_p^{\rm SI}$ as inputs to obtain different IceCube/DeepCore sensitivities to DM annihilation cross section on the $(m_\chi, \sigma_p^{\rm SI})$ plane for different annihilation channels. There are thus three scenarios for the input $\sigma_p^{\rm SI}$: (i) $\sigma_p^{\rm SI}$ favored by DAMA and CRESST-II; (ii) $\sigma_p^{\rm SI}$ bound set by XENON100; (iii) $\sigma_p^{\rm SI}$ bound set by XENON1T (2017) [31] assuming nondetection. We particularly compare IceCube sensitivity to $\langle\sigma(\chi\chi \to \tau^+\tau^-)v\rangle$ to the favored range on the same quantity implied by PAMELA, Fermi-LAT, and AMS02. It is seen that neither $\chi\chi \to W^+W^-$ nor $\chi\chi \to b\bar{b}$ can simultaneously fit well to PAMELA and AMS02 [12] if either channel is assumed to be dominant. We note that our work has assumed the dark matter interpretations for PAMELA, FERMI-LAT, and AMS02 data. The pulsar interpretations of these data are discussed in Ref. [32]. We conclude in Sec. V.

II. NEUTRINO FLUX FROM DM ANNIHILATION IN THE EARTH'S CORE

To facilitate our discussions, let us define $dN_{\nu_i}^f/dE_\nu$ as the energy spectrum of ν_i produced per DM annihilation $\chi\chi \to f\bar{f}$ in the Earth's core. The differential DM neutrino flux of flavor i on the Earth's surface is then given by

$$\frac{d\Phi_{\nu_i}^{\rm DM}}{dE_\nu} = P_{\nu_j\to\nu_i}(E_\nu, D)\frac{\Gamma_A}{4\pi D^2}\sum_f B_\chi^f \frac{dN_{\nu_j}^f}{dE_\nu}, \qquad (1)$$

where Γ_A is the DM annihilation rate, B_χ^f is the branching ratio for the DM annihilation channel $\chi\chi \to f\bar{f}$, D is the distance between the source and the detector, and $P_{\nu_j\to\nu_i}(E_\nu, D)$ is the neutrino oscillation probability from the source to the detector.

To calculate $d\Phi_{\nu_i}^{\rm DM}/dE_\nu$, we employ WIMPSIM [33] with a total of 50000 Monte Carlo generated events. Although we are particularly interested in IceCube/DeepCore measurements, the DM neutrino flux from the Earth core is the same for all detector locations near the Earth's surface due to the spherical symmetry. The oscillation probability $P_{\nu_j\to\nu_i}(E_\nu, D)$ is calculated

with the best-fit neutrino oscillation parameters summarized in Table I of Ref. [34], $\theta_{12} = 33.65^{\circ}$, $\theta_{13} = 8.93^{\circ}$, $\theta_{23} = 38.41^{\circ}$, $\delta = 1.08\pi$, $\delta m^2_{21} = 7.54 \times 10^{-5}$ eV^2, and $\delta m^2_{31} = 2.47 \times 10^{-3}$ eV^2.

The DM annihilation rate Γ_A can be determined by the following argument. When the Earth sweeps through DM halo, the WIMP could collide with matter inside the Earth and lose its speed. If the WIMP speed becomes less than its escape velocity, the WIMP can be captured by Earth's gravitational force and then sinks into the core of the Earth. After a long period of accumulation, WIMPs inside the core of the Earth can begin to annihilate into standard model particles at an appreciable rate. Among the annihilation final states, neutrinos can be detected by neutrino telescopes. Let $N(t)$ be the number of WIMPs in the Earth's core at time t, we have

$$\frac{dN}{dt} = C_c - 2\Gamma_A(t) - C_E N, \tag{2}$$

where C_c is the capture rate and C_E is the evaporation rate. It has been shown that WIMPS with masses between 5–10 GeV may evaporate from the Earth [26,28,35,36]. Since we are interested in the mass range $m_\chi > 10$ GeV, we neglect C_E in our discussions. The capture rate C_c depends on the DM-nuclei elastic scattering cross section which contains spin-dependent component $\sigma_p^{\rm SD}$ and spin-independent component $\sigma_p^{\rm SI}$. The DM annihilation rate $\Gamma_A(t)$ is proportional to $N^2(t)$. One writes

$$\Gamma_A(t) = \frac{1}{2} C_A N^2(t). \tag{3}$$

Taking into account the quasithermal distribution of WIMPs in the Earth's core, the annihilation coefficient C_A can be written as [37]

$$C_A = \frac{\langle \sigma_a v \rangle}{V_0} \left(\frac{m_\chi}{20\ \text{GeV}} \right)^{2/3}, \tag{4}$$

where $V_0 = 2.3 \times 10^{25}$ cm^3 for the Earth.

By solving $N(t)$ in Eq. (2), we obtain [36]

$$\Gamma_A(t) = \frac{C_c}{2} \tanh^2 \left(\frac{t}{\tau_A} \right), \tag{5}$$

where t is the age of the macroscopic body, for example $t = 4.5$ Gyr for the Sun and the Earth, while τ_A is the equilibration time scale, $\tau_A = (C_c C_A)^{-1/2}$. Numerically $\tanh^2(t/\tau_A) \to 1$ for $\frac{t}{\tau_A} > 2$. In such a case $\Gamma_A(t) = C_c/2$ so that the DM annihilation rate in the Earth's core depends only on the capture rate C_c and is independent of the annihilation cross section $\langle \sigma v \rangle$.

Since the heavy nuclei such as iron are abundant in the Earth's core, the capture cross section is enhanced due to its quadratic dependence on the nuclear atomic number. Therefore, the corresponding capture rate is given by [38]

$$C_c \propto \frac{\rho_0}{\text{GeV cm}^{-3}} \times \frac{\text{kms}^{-1}}{\bar{v}} \times \frac{\text{GeV}}{m_\chi} \times \frac{\sigma_p^{\rm SI}}{\text{pb}} \times \sum_A F_A^*(m_\chi), \tag{6}$$

with $\bar{v}$ the DM velocity dispersion, ρ_0 the local DM density, and A the atomic number of chemical element in the Earth's core. $F_A^*(m_\chi)$ is the product of various factors including the mass fraction of element A, the gravitational potential for element A, kinematic suppression factor, form factor, and a factor of reduced mass. The explicit form of $F_A^*(m_\chi)$ is not essential for our discussions. It can be found, for instance, in Ref. [38]. However, we like to stress that there are significant astrophysical uncertainties on the DM local density and its velocity distributions involved in C_c [39]. In this work, we use approximate formulas given in [38], which are adopted by DarkSUSY [40].

III. DM SIGNAL AND ATMOSPHERIC BACKGROUND EVENTS

Neutrino telescopes such as IceCube detect neutrinos by measuring muon track and cascade events, which are induced by neutrino-nucleon charged-current (CC) and neutral-current (NC) scatterings. We calculate neutrino event rate according to IceCube published neutrino effective area $A_{\rm eff}^{i,k}(E_\nu)$ [41] of the full IceCube 86-string detector, where k is the interaction type for different neutrino flavor i. For example, for muon track events, i is the (anti-) muon neutrino and k is the (anti-) muon neutrino CC interaction. On the other hand, for cascade events, i includes all three neutrino flavors. For (anti-) electron neutrinos and (anti-) tau neutrinos, k runs over CC and NC interactions while k is exclusively NC interaction for (anti-) muon neutrinos. The effective area accounts for the detection efficiency including the neutrino-nucleon interaction probability, the energy loss of muon from its production point to the detector, and the detector trigger, and analysis efficiency. Hence, the neutrino event rate from the Earth's DM is given by

$$N_{\rm signal} = \int_{E^{\rm th}}^{m_\chi} \sum_{i,k} \frac{d\Phi_{\nu_i}^{\rm DM}}{dE_\nu} A_{\rm eff}^{i,k}(E_\nu) dE_\nu d\Omega, \tag{7}$$

where $d\Phi_{\nu_i}^{\rm DM}/dE_\nu$ is the differential neutrino flux in the vicinity of detector for a given neutrino flavor i, which is given by Eq. (1), and the index k can be either NC or CC interaction. The effective area can be defined as $A_{\rm eff}^{i,k}(E_\nu) \approx \rho_{\rm ice} N_A \sigma_{\nu_i N}^k(E_\nu) V_{\rm eff}^{i,k}(E_\nu)$ [18], where $\rho_{\rm ice} = 0.9$ g/cm^3 is the density of ice, $N_A = 6.022 \times 10^{23}$ g^{-1} is the Avogadro number, $\sigma_{\nu_i N}^k(E_\nu)$ is the neutrino-nucleon cross-section, and $V_{\rm eff}^{i,k}(E_\nu)$ is the effective volume of IceCube for different neutrino-nucleon interaction events. In this work, we shall take the detector threshold energy Eth for IceCube/DeepCore as 10 and 100 GeV, respectively. To compute the rate for ν_μ track events, we shall

use the effective area (DeepCore+IceCube Trigger) given by Ref. [41].

Unlike the calculation of track event rate, which requires only one effective area, the calculation of cascade event rate requires 5 different effective areas. The cascade-event effective area given by Ref. [41] is only for ν_e CC interaction events. Here we also adopt the effective area marked as DeepCore + IceCube Trigger for estimating the ν_e event rate. To obtain effective areas for other cascade events, we perform the rescaling

$$A_{\rm eff}^{i,k}(E_\nu) = A_{\rm eff}^{\nu_e,{\rm CC}}(E_\nu) \times \frac{\sigma_{\nu_i N}^{k}(E_\nu)}{\sigma_{\nu_e N}^{\rm CC}(E_\nu)} \times \frac{V_{\rm eff}^{\nu_e,{\rm CC}}(\langle y\rangle \cdot E_\nu)}{V_{\rm eff}^{\nu_e,{\rm CC}}(E_\nu)}, \tag{8}$$

where $\langle y\rangle$ is the averaged fraction of neutrino energy E_ν converted into shower energy after a neutrino-nucleon CC or NC interaction. One has $\langle y\rangle = 0.3$ for NC interactions of ν_e and ν_μ while $\langle y\rangle = 1$ for ν_e CC interaction [42]. For ν_τ, the fraction $\langle y\rangle$ resulting from ν_τ CC interaction and subsequent tau-lepton decay is approximately $0.6 \times \langle y_h\rangle + 0.4$ where $\langle y_h\rangle$ is the energy fraction of ν_τ taken by hadrons in ν_τ-nucleon CC interaction [43]. The factor 0.4 is the visible energy fraction in tau lepton decays, which can be estimated by using PYTHIA [44]. It should be noted that the final effective area/effective volume for cascade events may be significantly reduced due to the background rejection cut. In a recent IceCube 79-string result on atmospheric ν_e flux measurement [45], the final effective volume for ν_e events is much smaller than the one at the DeepCore filter level for lower energies while such a difference is within an order of magnitude for $E_\nu \gtrsim 10^3$ GeV, as can be seen from Fig. 2 of that paper. Since our sensitivity calculations for cascade events are based upon effective areas in Ref. [41], we only present IceCube/DeepCore sensitivities for $E^{\rm th} = 100$ GeV in the case of cascade events.

For calculating the atmospheric (ATM) background event rates, we use the atmospheric neutrino flux taken from Ref. [46]. Because the intrinsic ATM ν_τ flux is negligible, we only consider ATM ν_e and ν_μ fluxes at the production point. It is essential to include the effect of neutrino transmissions through the Earth. Since the Earth becomes opaque to neutrinos only for $E_\nu > 40$ TeV [43], the neutrino transmission in our interested energy range is essentially the neutrino oscillation effect. Hence the ATM background event rate is given by

$$N_{\rm background} = \int_{E^{\rm th}}^{E_{\rm max}} \sum_{i,k} \frac{d\Phi_{\nu_i}^{\rm ATM}}{dE_\nu} A_{\rm eff}^{i,k}(E_\nu) dE_\nu d\Omega, \tag{9}$$

where $d\Phi_{\nu_i}^{\rm ATM}/dE_\nu$ is the ATM neutrino flux in the vicinity of the detector. Such a flux is given by

$$\frac{d\Phi_{\nu_i}^{\rm ATM}}{dE_\nu} = \frac{d\Phi_{0,\nu_j}^{\rm ATM}}{dE_\nu} P_{\nu_j \to \nu_i}(E_\nu, L(\theta_\nu)), \tag{10}$$

where $d\Phi_{0,\nu_j}^{\rm ATM}/dE_\nu$ is the ATM neutrino flux at the source, $P_{\nu_j\to\nu_i}(E_\nu, L(\theta_\nu))$ is the neutrino oscillation probability with $L(\theta_\nu)$ the neutrino traversing distance through the Earth along the direction of θ_ν. For comparison with the signal event rate induced by Earth's DM annihilation with DM mass m_χ, $E_{\rm max}$ is taken as m_χ in Eq. (9). We remark that $E_{\rm max}$ should differ from m_χ in practice due to the energy resolution effect. However, the impact of energy resolution on our sensitivity estimation will be shown insignificant in the next section.

In Fig. 1, we show the number of neutrino events in 5 years from DM annihilations ($\chi\chi \to \tau^+\tau^-$) and the ATM background as functions of the maximum open angle $\psi_{\rm max}$ (left) and the DM mass m_χ (right), respectively. We stress that $N_{\rm events}$ is the total number of neutrino events integrated from the detector threshold energy to the maximal energy m_χ. Such information is useful for later discussions. Here, we take $\langle\sigma v\rangle = 3\times10^{-26}$ cm^3 s^{-1} and $\sigma_p^{\rm SI}$ the 90% CL upper limit f rom XENON100. From Eq. (4), we can see the annihilation coefficient C_A is inversely proportional to a m_χ dependent effective volume $V_{\rm eff} = V_0(20\ {\rm GeV}/m_\chi)^{2/3}$, which describes the volume of dark matter occupation in the Earth's core. Hence it is seen from the left panel of Fig. 1 that $N_{\rm events}$ reaches to the maximum for sufficiently large $\psi_{\rm max}$ that can cover the entire DM populated region in the Earth's core. The critical value of $\psi_{\rm max}$ for covering the DM populated region in the Earth's core is a function of m_χ, which we denote as $\psi_{\rm max}^{\rm c}(m_\chi)$. We have

$$\psi_{\rm max}^{\rm c}(m_\chi) = \max\left[\sin^{-1}\left(\frac{1}{R_\oplus}\times\left(\frac{3V_{\rm eff}(m_\chi)}{4\pi}\right)^{\frac{1}{3}}\right), 1^\circ\right], \tag{11}$$

where $R_\oplus$ the radius of the Earth. The 1° on the right-hand side of the equation is to ensure a minimal open angle of 1°. We have seen that $V_{\rm eff}(m_\chi)$ decreases as m_χ increases. Hence, $\psi_{\rm max}^{\rm c}$ for $m_\chi = 500$ GeV is smaller than $\psi_{\rm max}^{\rm c}$ for $m_\chi = 50$ GeV, as can be seen from the left panel of Fig. 1. The right panel of Fig. 1 shows DM and ATM background event numbers as functions of m_χ where $\psi_{\rm max}$ for each m_χ is taken to be $\psi_{\rm max}^{\rm c}(m_\chi)$. The $N_{\rm events}$ for the ATM background should have been increasing with m_χ for a fixed $\psi_{\rm max}$ since the maximal energy for these neutrino events is taken to be m_χ. However, as just mentioned, we have taken $\psi_{\rm max}$ to be $\psi_{\rm max}^{\rm c}(m_\chi)$, which decreases with m_χ. As a result, $N_{\rm events}$ for the ATM background stays almost a constant over a wide range of m_χ. The $N_{\rm events}$ for DM signal peaks at three different values of m_χ. This is due to the enhancement of the capture rate when m_χ is close to the mass of any dominantly populated

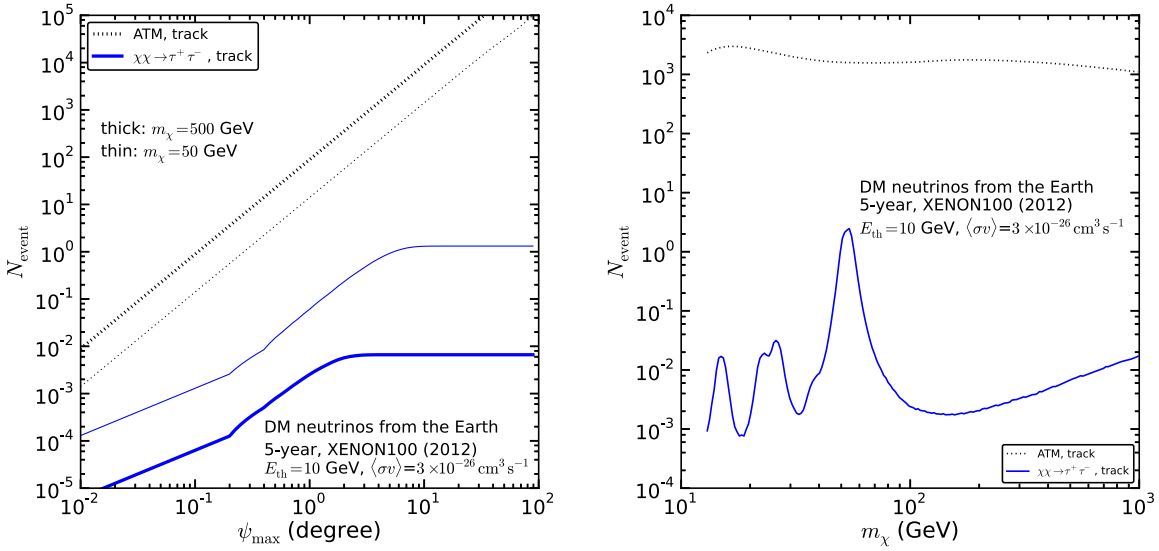

FIG. 1 (color online). The events collected in 5 years. We display the total events in the detector as function of $\psi_{\rm max}$ (left) and m_χ (right).

nuclei in the Earth's core. In fact, the three peaks from small to large m_χ correspond to the resonant capture by oxygen, Mg/Si, and Fe/Ni, respectively. Effects of these resonant capture peaks have been studied in inert doublet [47] and supersymmetry neutralino DM models [48,49]. In Ref. [50], the authors also included the effect from dark disc and found that the search for DM annihilation in the Earth can have the same level of sensitivity as the search for DM annihilation in the Sun for $m_\chi \lesssim 100$ GeV.

IV. RESULT

We present the sensitivity as a 2σ detection significance in 5 years, calculated with the standard formula

$$\frac{\text{DM signal}}{\sqrt{\text{ATM background}}} = 2.0. \tag{12}$$

The ATM here is the number of atmospheric background events, which we calculate with the flux data from Ref. [46]. The right-hand side of Eq. (12)) refers to the 2σ detection significance.

As mentioned earlier, the effect of detector energy resolution on the sensitivity estimation needs to be understood. The energy resolution for muon track events in IceCube/DeepCore can be parametrized as $(\sigma_E/\text{GeV})^2 = 5^2 + (0.2 \cdot E/\text{GeV})^2$ [51], while the energy resolution for cascade events can reach to $\Delta(\log_{10}(E/\text{GeV})) = 0.1$ [52]. Here we take a conservative energy resolution $\sigma_E/E = 50\%$, which is roughly the resolution for track events near the threshold energy $E_{\rm th} = 10$ GeV. One expects the energy resolution of neutrino events to be significantly improved in the liquid scintillation detector, which could measure the direction and energy of the recoiling nucleon from scintillation light [53–55]. With $\sigma_E/E = 50\%$, we may compare the ATM track event rate in Eq. (9) with $E_{\rm max} = m_\chi$ and the similar event rate with $E_{\rm max} = 3m_\chi/2$, which has taken into account the 50% energy resolution. We have found that, for $E^{\rm th} = 10$ GeV and $12 < E_{\rm max}/\text{GeV} < 10^3$, the ratio of the ATM background event rate with $E_{\rm max} = 3m_\chi/2$ to that with $E_{\rm max} = m_\chi$ varies between 2.7 and unity. From Eq. (12), we can see that the magnitude of DM annihilation cross section which the detector can probe is proportional to the square root of the ATM background event number. Thus the IceCube sensitivity to $\langle\sigma v\rangle$ with track events is changed only slightly by a factor f in the range $1 < f < 1.65$. We expect a similar effect for cascade events. Therefore, the effect of energy resolution on our sensitivity estimation is insignificant.

In Fig. 2, we show the 5 year sensitivity of the full IceCube 86-string detector to Earth's DM signal on $(\langle\sigma v\rangle,\ \sigma_p^{\rm SI})$ plane. We consider annihilation channels $\chi\chi \to \nu_e\bar{\nu}_e$, $\nu_\mu\bar{\nu}_\mu$, and $\tau^+\tau^-$. The first annihilation mode produces cascade events while the second and third channels produce both track and cascade events due to $\nu_\mu \to \nu_\tau$ oscillations. Each annihilation channel is assumed to be dominant when IceCube/DeepCore sensitivity to that channel is derived. We note that the branching fraction for monochromatic channel $\chi\chi \to \nu\bar{\nu}$ can be sizeable or even dominant in certain DM models [56–58]. The uncertainty on the angle between the incoming neutrino and the outgoing charged lepton directions in neutrino-nucleon CC interaction sets the lower limit for the open angle $\psi_{\rm max}$. The above uncertainty can be approximated by $\Delta\phi \simeq 30^\circ \times \sqrt{(1\ \text{GeV})/E_\nu}$ [59]. We have taken the open angle $\psi_{\rm max}$ for

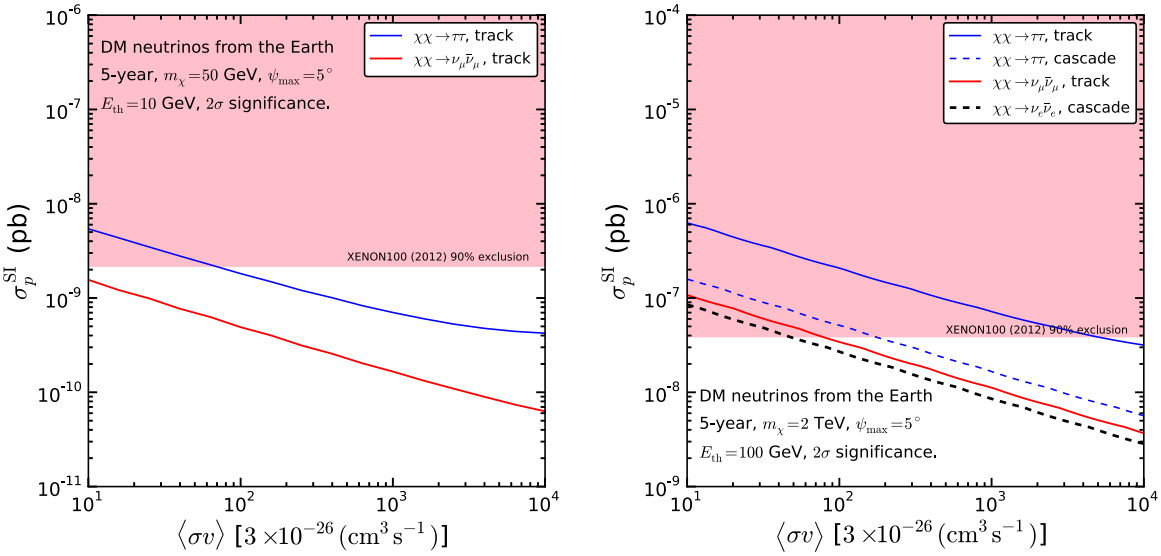

FIG. 2 (color online). The 5 year sensitivity in 2σ significance on the $(\langle\sigma v\rangle, \sigma_p^{\rm SI})$ plane. In the left panel, the DM mass is 50 GeV and the threshold energy is 10 GeV. The DM mass is 2 TeV and threshold energy is taken to be 100 GeV in the right panel. Solid lines are sensitivities with track events while dashed lines are sensitivities with cascade events. The pink shaded area represents the 90% exclusion from XENON100 (2012) result.

collecting events from the Earth's core to be 5° for both track and cascade events. For track events, this choice is slightly optimistic for events near the threshold energy $E_{\rm th} = 10$ GeV in the left panel. However, it is reasonable for all track events in the right panel with $E_{\rm th} = 100$ GeV. For the former case, a more realistic choice for $\psi_{\rm max}$ will also be taken in our later discussions. For cascade events, we only consider high threshold energy $E_{\rm th} = 100$ GeV which is presented in the right panel. Hence the above choice for $\psi_{\rm max}$ is also achievable for cascade events according to the angular resolution study in Ref. [60]. We note that the angular resolution for neutrino events can be significantly improved in the liquid scintillation detectors mentioned above [53–55], since the direction and energy of the recoiling nucleon can be measured in such type of detectors.

In the right panel of Fig. 2, we can see that $\chi\chi \to \nu_e\bar{\nu}_e$ channel is most sensitive to $\sigma_p^{\rm SI}$. In particular, this channel provides a better sensitivity to $\sigma_p^{\rm SI}$ than $\chi\chi \to \nu_\mu\bar{\nu}_\mu$ does, i.e., one can probe $\chi\chi \to \nu_e\bar{\nu}_e$ to a regime of smaller event rates. This is true since the ν_e cascade background event rate for the former channel is suppressed compared to the ν_μ track background event rate for the latter channel.

We note that the 5 year sensitivity curve on $(\langle\sigma v\rangle, \sigma_p^{\rm SI})$ plane is almost linear in logarithmic scale so that $\sigma_p^{\rm SI}$ approximates to $\langle\sigma v\rangle^{-k}$ with slope $-k$. As $\langle\sigma v\rangle$ increases, a smaller scattering cross section $\sigma_p^{\rm SI}$ is sufficient to achieve the same detection significance. However, Eq. (3) implies that this trend cannot continue indefinitely. As $\tanh(\frac{t}{\tau_A})$ is driven to the plateau by a sufficiently large $\langle\sigma v\rangle$, C_c must approach to a constant value for maintaining the same annihilation rate Γ_A. This then implies that $\sigma_p^{\rm SI}$ also approaches to a constant value. In the reverse direction where $\langle\sigma v\rangle$ decreases, a larger $\sigma_p^{\rm SI}$ is required to achieve the same detection significance. On the other hand, the XENON100 limit (pink shaded region) eventually sets the upper bound for $\sigma_p^{\rm SI}$. This constraint is clearly seen for the $\chi\chi \to \tau^+\tau^-$ channel with $m_\chi = 2$ TeV. Due to the XENON100 limit, such a channel cannot produce enough neutrino events in IceCube for reaching 2σ sensitivity in 5 years, unless the boost factor for $\langle\sigma v\rangle$ is larger than 1000.

It is clear that the XENON100 limit sets a m_χ-dependent bound on $\langle\sigma v\rangle$ for each annihilation channel. However, if one takes different experimental bounds on $\sigma_p^{\rm SI}$, the prospect of observing neutrinos from the Earth's core differs drastically. There are thus three possibilities:

Case A: Neutrino observation implied by DAMA and CRESST-II favored parameter space;

Case B: $\langle\sigma v\rangle$ exclusion limits implied by the XENON100 bound on $\sigma_p^{\rm SI}$;

Case C: Pessimistic scenario by assuming nondetection of XENON1T (2017).

Below we shall discuss in turn these three cases.

A. Neutrino observation implied by DAMA and CRESST-II

In Fig. 3, we present IceCube/DeepCore sensitivities to $\chi\chi \to \tau^+\tau^-$, W^+W^-, and $b\bar{b}$ annihilations in the Earth's core on the $(m_\chi, \sigma_p^{\rm SI})$ plane for track events with different $\psi_{\rm max}$ and $\langle\sigma v\rangle$ with $E^{\rm th} = 10$ GeV. The sensitivities to $\chi\chi \to W^+W^-$ (black dashed-doted) and $\chi\chi \to \tau^+\tau^-$ (grey solid) are comparable, albeit the W^+W^- channel only opens at $m_\chi > m_W$. The experimental upper limits of

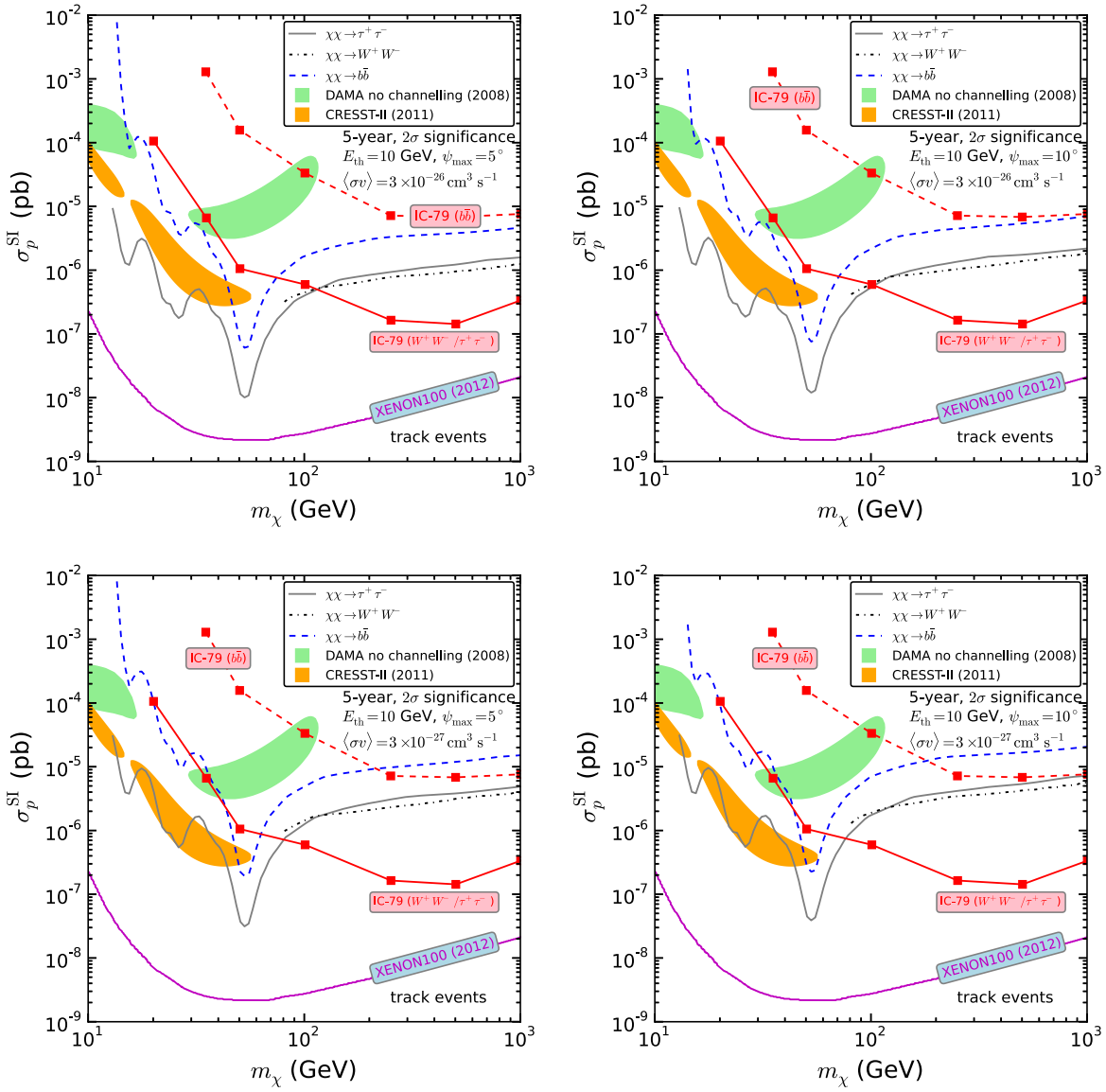

FIG. 3 (color online). The IceCube/DeepCore 5 year sensitivity curves on the (m_χ, $\sigma_p^{\rm SI}$) plane for $\chi\chi \to \tau^+\tau^-$, W^+W^-, and $b\bar{b}$ annihilation channels. The upper figures are based on $\langle\sigma v\rangle = 3\times10^{-26}$ cm^3 s^{-1} while the lower figures are based on $\langle\sigma v\rangle = 3\times10^{-27}$ cm^3 s^{-1}. The track-event sensitivities with $\psi_{\rm max} = 5^\circ$ are presented in figures on the left column and that with $\psi_{\rm max} = 10^\circ$ are presented in figures on the right column. The energy threshold is taken to be 10 GeV. The IceCube 79-string upper limits on $\chi\chi \to b\bar{b}$ (red dashed-squared line) and $\chi\chi \to W^+W^-/\tau^+\tau^-$ (red solid-squared line) from the search for DM-induced neutrino signature from the Sun are also shown for comparison [61].

$\chi\chi \to b\bar{b}$ (red dashed-squared line) and $\chi\chi \to W^+W^-/\tau^+\tau^-$ (red solid-squared line) are taken from the IceCube 79-string result on the search for muon neutrino events induced by DM annihilations in the Sun [61]. The IceCube 79-string result is based upon one year (317 days) of data between June 2010 and May 2011. We note that the constraint on $\chi\chi \to W^+W^-/\tau^+\tau^-$ stands for a constraint on $\chi\chi \to W^+W^-$ for $m_\chi > m_W$ and a constraint on $\chi\chi \to \tau^+\tau^-$ for $m_\chi < m_W$. For $m_\chi \lesssim 100$ GeV, it is seen that the 5-year IceCube/DeepCore sensitivity to $\sigma_p^{\rm SI}$ from detecting DM annihilations in the Earth's core is stronger than the above IceCube 1-year bound from detecting DM annihilations in the Sun. In fact, the former sensitivity to $\sigma_p^{\rm SI}$ remains stronger than the latter constraint even with just one year of data. Since the 1-year sensitivity is $\sqrt{5}$ times weaker than the 5-year sensitivity, our calculated $\sigma_p^{\rm SI}$ sensitivity curves can be easily scaled up for describing the 1-year sensitivity.

The favored region of DAMA at higher m_χ is not compatible with the IceCube 79-string constraint on $\chi\chi \to \tau^+\tau^-$. This region can also be probed by searching for neutrinos from $\chi\chi \to \tau^+\tau^-$ and $b\bar{b}$ annihilations in the Earth's core. In fact, the search for muon track events induced by $\chi\chi \to \tau^+\tau^-$ with $\langle\sigma v\rangle = 3\times10^{-26}$ cm^3 s^{-1} can

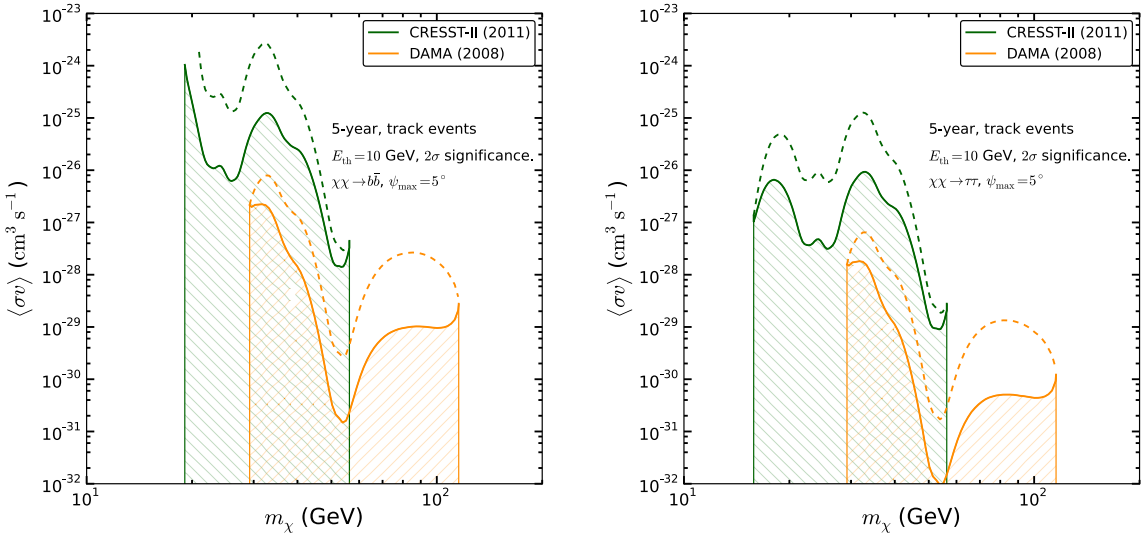

FIG. 4 (color online). The IceCube/DeepCore 5 year track-event sensitivity curves in 2σ significance on the $(m_\chi,\langle\sigma v\rangle)$ plane for $E_{\rm th}=10$ GeV and $\psi_{\rm max}=5^\circ$. The $\sigma_p^{\rm SI}$ input values are taken from no channeling DAMA and CRESST-II shown in Fig. 3. The figure in the left panel is for $\chi\chi\to b\bar{b}$ channel while the figure on the right panel is for $\chi\chi\to\tau^+\tau^-$ channel. The dashed/solid lines correspond to sensitivities obtained with input $\sigma_p^{\rm SI}$ given by the lower/upper boundary of DAMA and CRESST contours. The allowed regions for $\langle\sigma v\rangle$ are indicated by hatched areas.

probe the full allowed region of DAMA and most of the allowed region of CRESST-II. With a 10 times smaller $\langle\sigma v\rangle$, the full allowed region of DAMA can still be probed by the same annihilation channel.

From Fig. 2, we can see that the sensitivity is correlated as $\sigma_p^{\rm SI}\sim\langle\sigma v\rangle^{-k}$. Therefore, if one takes DAMA and CRESST-II favored regions as input, it is possible to probe $\langle\sigma v\rangle$ to a value much smaller than 3×10^{-26} cm^3 s^{-1} as shown by Fig. 4. In this figure, it is assumed that DM parameter regions are those given by DAMA and CRESST-II. We then present the IceCube/DeepCore 5 year track-event sensitivity curves on the $(m_\chi,\langle\sigma v\rangle)$ plane. We take the boundary of the discovery contour of DAMA and CRESST-II as our $\sigma_p^{\rm SI}$ inputs. The upper IceCube/DeepCore sensitivity curves (thin lines) are driven by the lower boundary of $\sigma_p^{\rm SI}$ contours of DAMA and CRESST-II, while the lower sensitivity curves (thick lines) are driven by the upper boundary of $\sigma_p^{\rm SI}$ contours. We do not use the data of CoGent because their favored DM mass range is below the energy threshold $E_{\rm th}=10$ GeV. For the same reason, we also ignore the $m_\chi<15$ GeV favored regions of DAMA and CRESST-II. We choose the open angle $\psi_{\rm max}=5^\circ$. Because of the large capture rate C_c resulted from the iron resonance region, $\langle\sigma v\rangle$ for this m_χ range can be probed to values much smaller than the thermal average cross section $\langle\sigma v\rangle\sim3\times10^{-26}$ cm^3 s^{-1}.

B. $\langle\sigma v\rangle$ exclusion limits implied by XENON100 bound on $\sigma_p^{\rm SI}$

We can take the XENON100 90% upper limit as the input $\sigma_p^{\rm SI}$. Let us begin by taking $E^{\rm th}=10$ GeV and consider only track events. The 5-year IceCube/DeepCore 2σ sensitivities to $\langle\sigma(\chi\chi\to\nu_\mu\bar{\nu}_\mu)v\rangle$ and $\langle\sigma(\chi\chi\to\tau^+\tau^-)v\rangle$ as functions of m_χ are presented in Fig. 5. We note that the annihilation channel $\chi\chi\to\tau^+\tau^-$ can give rise to

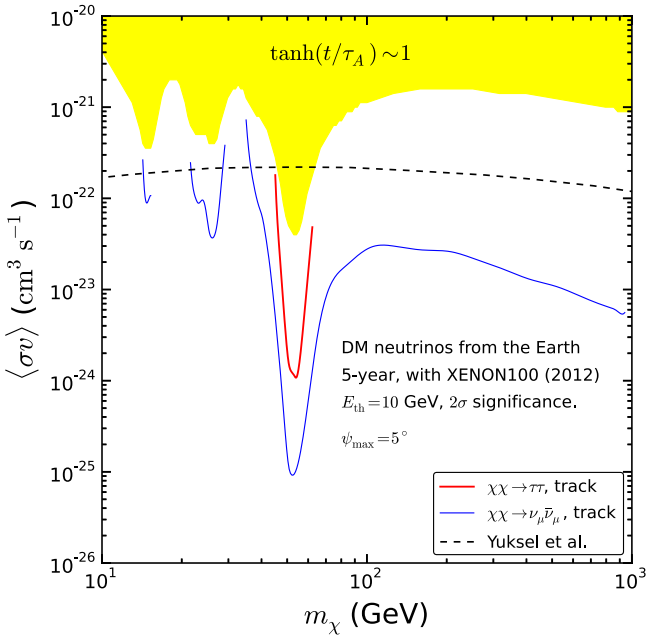

FIG. 5 (color online). The 5-year IceCube/DeepCore 2σ sensitivities to $\langle\sigma(\chi\chi\to\nu_\mu\bar{\nu}_\mu)v\rangle$ and $\langle\sigma(\chi\chi\to\tau^+\tau^-)v\rangle$ as functions of m_χ with track events. The $\sigma_p^{\rm SI}$ is taken from the XENON100 90% upper limit. The yellow shaded area corresponds to the steady state with $\tanh(\frac{t}{\tau_A})\sim1$. We take $E^{\rm th}=10$ GeV and $\psi_{\rm max}=5^\circ$. The bound on $\chi\chi\to\nu\bar{\nu}$ annihilation cross section [62] using the data of Fréjus, Super-Kamiokande, and AMANDA detectors is also shown.

track events due to the $\nu_\tau \to \nu_\mu$ oscillations for lower E_ν. The results are obtained by considering track events with $\psi_{\max} = 5^\circ$. The yellow shaded region corresponds to the steady state with $\tanh(\frac{t}{\tau_A}) \sim 1$, which is caused by a sufficiently large $\langle \sigma v \rangle$ when $\sigma_p^{\rm SI}$ is fixed at the current XENON100 upper limit. In this case, the number of DM trapped in the Earth's core reaches to the equilibrium value since $\Gamma_A = C_c/2$. As a result, the annihilation rate which dictates the neutrino flux is determined entirely by the capture rate and is independent of $\langle \sigma v \rangle$. The latter only determines the number of DM in the equilibrium. Hence the measurement of neutrino flux in the steady state can only determine $\sigma_p^{\rm SI}$.

We can see the strongest limit comes from the iron resonance region $m_\chi \sim 50$ GeV where the capture rate C_c peaks. On the other hand, the weakest bound of $\langle \sigma v \rangle$ occurs at the lowest point of the XENON100 $\sigma_p^{\rm SI}$ upper limit located at $m_\chi \sim 100 - 200$ GeV. Moreover, the curves are broken near the boundary of the yellowed region. Hence, for each annihilation channel, there exists a range of m_χ where the 2σ significance curve disappears. This means that the DM event number in this m_χ range cannot reach the 2σ significance before $\langle \sigma v \rangle$ reaches to the steady state $\tanh(\frac{t}{\tau_A}) \sim 1$. One should bear in mind that this yellowed region varies with the input $\sigma_p^{\rm SI}$. Before we move on, it is instructive to compare our derived sensitivities

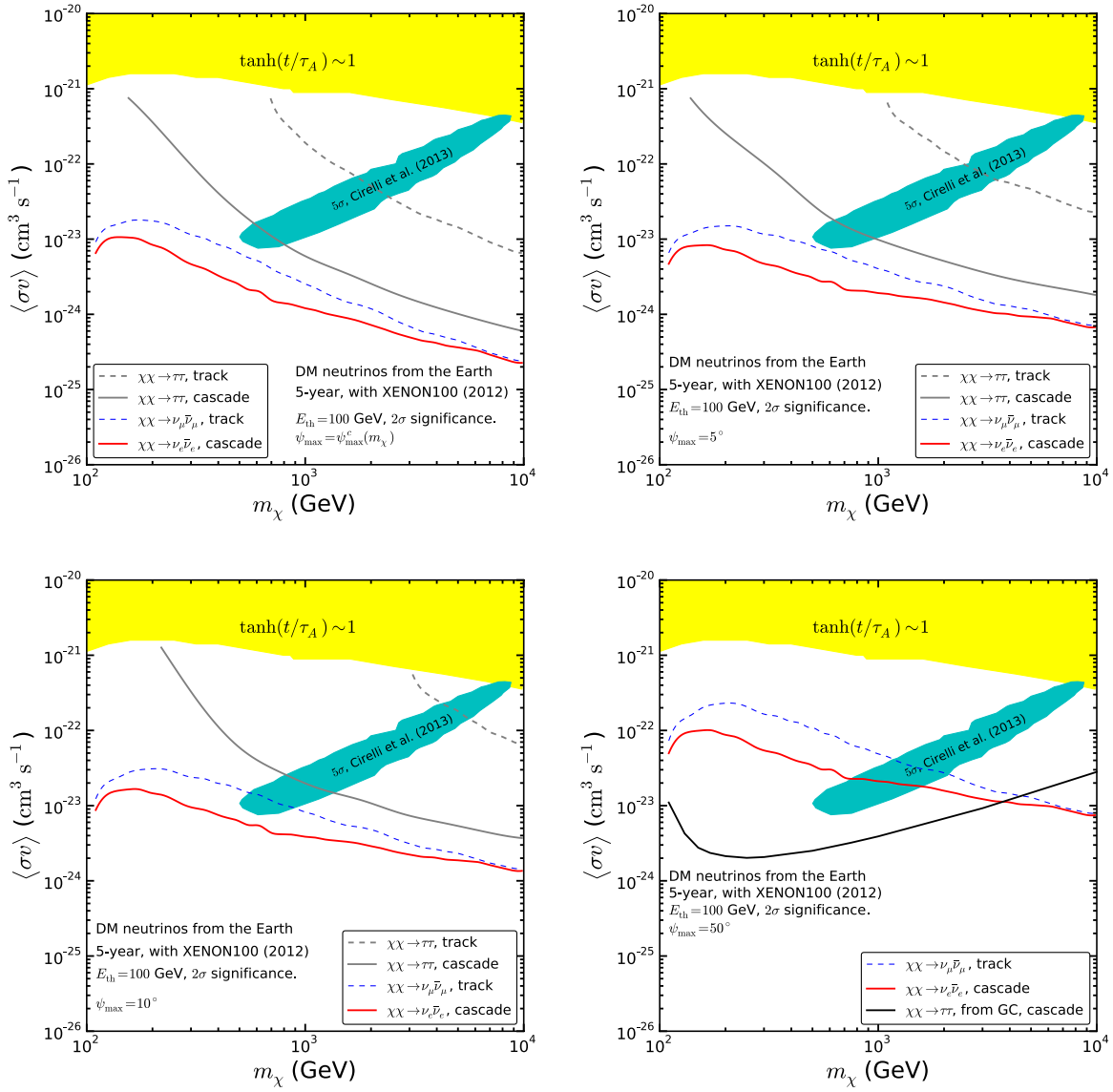

FIG. 6 (color online). The 5-year IceCube/DeepCore 2σ sensitivities to $\langle \sigma v \rangle$ of various channels as functions of m_χ with track and cascade events. The threshold energy is taken to be 100 GeV and the m_χ range is extended to 10 TeV. The cyan contours refer to 5σ confidence region of PAMELA and AMS02 combined analysis, for $\chi\chi \to \tau^+\tau^-$ channel, taken from Ref. [9]. The black solid line is the 5 year sensitivity upper limit of $\langle \sigma(\chi\chi \to \tau^+\tau^-)v \rangle$ in 2σ significance obtained from the search of neutrino cascade events from the galactic center with $\psi_{\max} = 50^\circ$ relative to the direction of galactic center.

to existing bounds on the DM annihilation cross section in the galactic halo. These bounds were derived some time ago [62] by comparing the expected neutrino spectrum from DM annihilations in the galactic halo with the well-measured atmospheric neutrino spectrum by Fréjus, Super-Kamiokande, and AMANDA detectors [63]. We show one of those bounds on the $\chi\chi \to \nu\bar{\nu}$ annihilation cross section in Fig. 5 for comparison. Such a bound is referred to as *Milky Way Halo Average* by the authors, which considers the average of DM distribution integrated over the line-of-sight for the entire sky. It is seen that the current IceCube/DeepCore detector can probe into a much smaller DM annihilation cross section compared to neutrino detectors mentioned above.

We next take $E^{\rm th} = 100$ GeV and consider both track and cascade events. We present in Fig. 6 the IceCube/DeepCore sensitivities to $\langle\sigma v\rangle$ of various channels as functions of m_χ. The result in the upper left panel is obtained by taking $\psi_{\rm max} = \psi^{\rm c}_{\rm max}(m_\chi)$, while $\psi_{\rm max}$ is taken to be 5°, 10°, and 50° for results in the upper right, lower left, and lower right panels, respectively. For the $\chi\chi \to \tau^+\tau^-$ channel, we also plot the 5σ confidence region favored by PAMELA and AMS02 positron fraction data [9] for comparison. One can see that the search for $\chi\chi \to \tau^+\tau^-$ cascade events can probe almost all the 5σ favored region by PAMELA and AMS02 with $\psi_{\rm max} = 5^\circ$. For comparison, we also estimate the IceCube/DeepCore sensitivity to the DM annihilation cross section in the galactic halo with a 100 GeV threshold energy by using the method of Ref. [24] and the energy-dependent effective volume $V_{\rm eff}(E)$ [41]. The 5 year sensitivity upper limit of $\langle\sigma(\chi\chi \to \tau^+\tau^-)v\rangle$ obtained from searching for neutrino cascade events from the galactic center with $\psi_{\rm max} = 50^\circ$ relative to the direction of the galactic center is also plotted. We note that this sensitivity is independent of $\sigma_p^{\rm SI}$, unlike the search for DM annihilations in the Earth's core. One can see that the search for galactic DM annihilations by IceCube/DeepCore can probe the entire 5σ confidence region favored by PAMELA and AMS02 in 5 years of running. We note the idea of using DM-induced neutrinos from the galactic center to examine the PAMELA and FERMI favored parameter space was first proposed in Refs. [17–19].

It is interesting to note that $\chi\chi \to \tau^+\tau^-$ at the current energy range also produces track events since a tau lepton can decay into muon neutrinos. In Fig. 7, we summarize the sensitivities with track events for the $\tau^+\tau^-$ channel with different open angles, $\psi_{\rm max} = 1^\circ$ (red solid), 2° (green dashed-dot), 5° (black dot), 10° (grey solid), and $\psi_{\rm max} = \psi^{\rm c}_{\rm max}(m_\chi)$ (blue dashed). We note that the sensitivity curves for $\psi_{\rm max} = 1^\circ$ and 2° cross at $m_\chi \sim 600$ GeV. In other words, for $m_\chi < 600$ GeV, the numerator in Eq. (12) increases faster than the denominator as $\psi_{\rm max}$ increases from 1° to 2° (see the left panel of Fig. 1). Moreover, we note that the sensitivity to $\langle\sigma v\rangle$ can change by more than one order

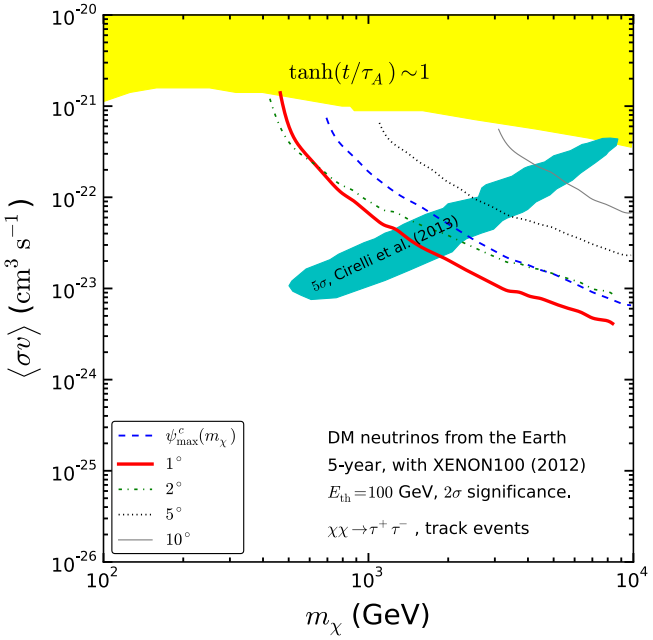

FIG. 7 (color online). The IceCube/DeepCore sensitivities to $\langle\sigma(\chi\chi \to \tau^+\tau^-)v\rangle$ with track events for several different open angles.

of magnitude as the open angle $\psi_{\rm max}$ increases from 1° to 10°. Finally, with $\psi_{\rm max} = 1^\circ$, IceCube 5 year data can probe the PAMELA and AMS02 positron favored region for $m_\chi \gtrsim 2$ TeV.

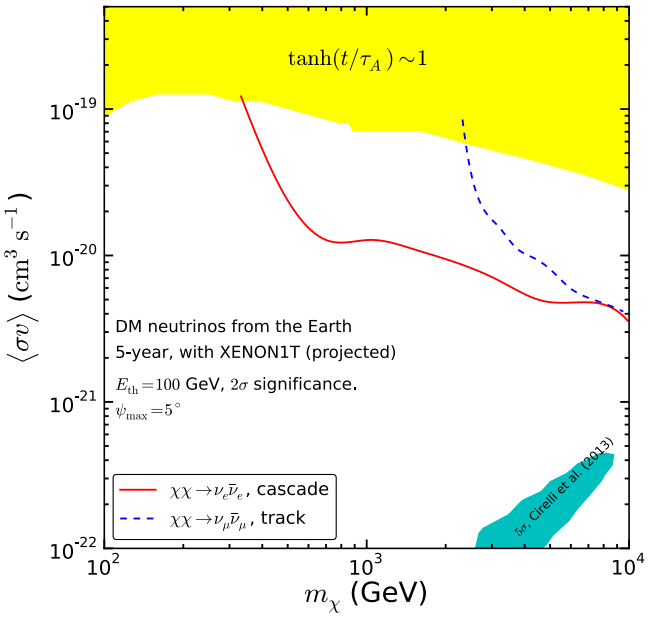

FIG. 8 (color online). The IceCube/DeepCore 5 year sensitivity with 2σ significance on the $(m_\chi, \langle\sigma v\rangle)$ plane. The $\sigma_p^{\rm SI}$ input is taken from the XENON1T sensitivity curve. We take $\psi_{\rm max} = 5^\circ$. The threshold energy is taken to be 100 GeV. The red solid line and blue dashed line are IceCube sensitivities to $\chi\chi \to \nu_e\bar{\nu}_e$ cascade events and $\chi\chi \to \nu_\mu\bar{\nu}_\mu$ track events, respectively.

C. Pessimistic scenario by assuming nondetection of XENON1T (2017)

Finally we discuss a pessimistic scenario that DM is not detected by XENON1T (a future ton-size DM detector). In Fig. 8, instead of using the current XENON100 limit as the input for $\sigma_p^{\rm SI}$, we compute the IceCube 5-year 2σ sensitivity upper limit with the projected $\sigma_p^{\rm SI}$ limit from XENON1T [31] as the input. We set the threshold energy at 100 GeV and present our result for m_χ up to 10 TeV. Even if XENON1T $\sigma_p^{\rm SI}$ sensitivity limits at larger m_χ are weaker, only those $\langle\sigma v\rangle$ arising from monochromatic annihilation channels can be probed by IceCube, i.e., by observing cascade events from $\chi\chi \to \nu_e\bar{\nu}_e$ and $\chi\chi \to \nu_\tau\bar{\nu}_\tau$ channels (not shown on the figure), and by observing track events from $\chi\chi \to \nu_\mu\bar{\nu}_\mu$ channel. However this upper limit is not stringent since the strongest bound for $\langle\sigma v\rangle$ in this case is roughly 10^{-22} cm^3 s^{-1}.

V. SUMMARY AND CONCLUSIONS

In this paper, we study the neutrino signature arising from DM annihilations inside the Earth's core. Applying IceCube/DeepCore effective areas, we have computed IceCube/DeepCore 5-year sensitivities in 2σ significance with track and cascade events. We note that our sensitivity calculations based upon Eq. (12) should be viewed as approximations. In actual experimental analysis, detailed Monte Carlo studies of systematic uncertainties are involved. From the slope of sensitivity curves in Fig. 2, it is seen that the neutrino event rate is more sensitive to $\sigma_p^{\rm SI}$ than $\langle\sigma v\rangle$. To illustrate the impact of $\sigma_p^{\rm SI}$ on the neutrino event rate, we have focused on three different scenarios according to different input $\sigma_p^{\rm SI}$. Hence our results can be divided by three categories.

A. Implications from $\sigma_p^{\rm SI}$ favored by DAMA and CRESST II

We have compared the 5-year full IceCube/DeepCore sensitivity to $\sigma_p^{\rm SI}$ derived from the search for DM annihilations in the Earth's core with the recent limit on $\sigma_p^{\rm SI}$ by the IceCube 79-string detector search for DM annihilations in the Sun. We found that the small DM mass region, $m_\chi \lesssim 100$ GeV, can be better probed by detecting DM annihilations in the Earth's core. By fixing $\langle\sigma v\rangle = 3\times10^{-26}$ cm^3 s^{-1}, we found that our $\tau^+\tau^-$ track event result can probe the entire DAMA allowed region and most of the CRESST-II allowed region. If one takes the large $\sigma_p^{\rm SI}$ favored by DAMA and CRESST-II as input, a rather low $\langle\sigma v\rangle$ is sufficient for IceCube/DeepCore to achieve 2σ detection significance in 5 years on DM annihilations in the Earth's core. It will be quite a challenge for other indirect detection experiments to achieve such a sensitivity to $\langle\sigma v\rangle$ in the near future.

B. Implication from $\sigma_p^{\rm SI}$ bound set by XENON100:

We have also considered the scenario of taking the current XENON100 bound as our input $\sigma_p^{\rm SI}$. We have discussed the implications by taking $E^{\rm th}$ as 10 and 100 GeV, respectively. In the former case, we study the IceCube/DeepCore sensitivities for m_χ up to 1 TeV and consider only track events. In the latter case, the IceCube/DeepCore sensitivities are studied for m_χ up to 10 TeV with both track and cascade events.

For $E_{\rm th} = 10$ GeV, we found that the strongest limit of $\langle\sigma v\rangle$ comes from the iron resonance region $m_\chi \sim 50$ GeV. Among all the DM annihilation channels, the most stringent limit with track events arises from $\chi\chi \to \nu_\mu\bar{\nu}_\mu$ annihilation.

For $E_{\rm th} = 100$ GeV where both track and cascade events are considered, the most stringent limit of $\langle\sigma v\rangle$ is from $\chi\chi \to \nu_e\bar{\nu}_e$ cascade events. Moreover, we have compared the IceCube/DeepCore sensitivities on the $(m_\chi, \langle\sigma v\rangle)$ plane with the parameter range favored by PAMELA and AMS02 data. We found that both track and cascade events in the $\chi\chi \to \tau^+\tau^-$ annihilation channel can test the PAMELA and AMS02 favored parameter space. With $\psi_{\rm max} = 1^\circ$, the search for DM induced neutrino track events from the Earth's core can rule out the PAMELA and AMS02 favored parameter region at $m_\chi \gtrsim 2$ TeV.

C. Implication of future XENON1T sensitivity

We finally discussed the pessimistic scenario that DM is not discovered by the future XENON1T. With an input $\sigma_p^{\rm SI}$ given by XENON1T sensitivity, we again discuss the implication on neutrino search.

With $E^{\rm th} = 100$ GeV and $10^2 < m_\chi/{\rm GeV} < 10^4$, we found that only those $\langle\sigma v\rangle$ arising from monochromatic annihilation channels, $\chi\chi \to \nu\bar{\nu}$, can be probed by IceCube in 5 years of data taking. However the expected bound on $\langle\sigma v\rangle$ by IceCube is disfavored by the current AMS-02 positron flux result.

ACKNOWLEDGMENTS

F. F. L. is supported by the grant from Research and Development Office, National Chiao-Tung University, G. L. L. is supported by National Science Council of Taiwan under Grant No. 99-2112-M-009-005-MY3 and National Center for Theoretical Sciences (NCTS), Taiwan, and Y. S. T. is funded in part by the Welcome Programme of the Foundation for Polish Science. Y. S. T. also likes to thank NCTS for hospitality during his visit.

[1] R. Bernabei *et al.* (DAMA and LIBRA Collaborations), Eur. Phys. J. C **67**, 39 (2010).
[2] C. E. Aalseth *et al.* (CoGeNT Collaboration), Phys. Rev. Lett. **106**, 131301 (2011).
[3] M. Bravin *et al.* (CRESST- Collaboration), Astropart. Phys. **12**, 107 (1999).
[4] E. Aprile *et al.* (XENON100 Collaboration), Phys. Rev. Lett. **109**, 181301 (2012).
[5] R. Agnese *et al.* (CDMS Collaboration), arXiv:1304.4279 [Phys. Rev. Lett. (to be published)].
[6] O. Adriani *et al.* (PAMELA Collaboration), Phys. Rev. Lett. **106**, 201101 (2011).
[7] M. Ackermann *et al.* (Fermi LAT Collaboration), Phys. Rev. D **82**, 092004 (2010).
[8] M. Aguilar *et al.* (AMS Collaboration), Phys. Rev. Lett. **110**, 141102 (2013).
[9] M. Cirelli, M. Kadastik, M. Raidal, and A. Strumia, Nucl. Phys. **B813**, 1 (2009).
[10] J. Kopp, Phys. Rev. D **88**, 076013 (2013).
[11] A. De Simone, A. Riotto, and W. Xue, J. Cosmol. Astropart. Phys. 05 (**2013**) 003.
[12] Q. Yuan, X.-J. Bi, G.-M. Chen, Y.-Q. Guo, S.-J. Lin, and X. Zhang, arXiv:1304.1482.
[13] I. Cholis and D. Hooper, Phys. Rev. D **88**, 023013 (2013).
[14] H.-B. Jin, Y.-L. Wu, and Y.-F. Zhou, J. Cosmol. Astropart. Phys. 11 (**2013**) 026.
[15] Q. Yuan and X.-J. Bi, Phys. Lett. B **727**, 1 (2013).
[16] M. Ackermann *et al.* (Fermi-LAT Collaboration), Phys. Rev. D **86**, 022002 (2012).
[17] D. Spolyar, M. R. Buckley, K. Freese, D. Hooper, and H. Murayama, arXiv:0905.4764.
[18] M. R. Buckley, D. Spolyar, K. Freese, D. Hooper, and H. Murayama, Phys. Rev. D **81**, 016006 (2010).
[19] S. K. Mandal, M. R. Buckley, K. Freese, D. Spolyar, and H. Murayama, Phys. Rev. D **81**, 043508 (2010).
[20] L. Covi, M. Grefe, A. Ibarra, and D. Tran, J. Cosmol. Astropart. Phys. 04 (**2010**) 017.
[21] A. E. Erkoca, M. H. Reno, and I. Sarcevic, Phys. Rev. D **82**, 113006 (2010).
[22] R. Abbasi *et al.* (IceCube Collaboration), Phys. Rev. D **84**, 022004 (2011).
[23] F.-F. Lee and G.-L. Lin, Phys. Rev. D **85**, 023529 (2012).
[24] F.-F. Lee, G.-L. Lin, and Y.-L. S. Tsai, Phys. Rev. D **87**, 025003 (2013).
[25] K. Freese, Phys. Lett. **167B**, 295 (1986).
[26] A. Gould, Astrophys. J. **321**, 571 (1987).
[27] J. Lundberg and J. Edsjo, Phys. Rev. D **69**, 123505 (2004).
[28] L. M. Krauss, M. Srednicki, and F. Wilczek, Phys. Rev. D **33**, 2079 (1986).
[29] I. F. M. Albuquerque, L. J. Beraldo e Silva, and C. Perez de los Heros, Phys. Rev. D **85**, 123539 (2012).
[30] C. Delaunay, P. J. Fox, and G. Perez, J. High Energy Phys. 05 (**2009**) 099.
[31] E. Aprile (XENON1T Collaboration), arXiv:1206.6288.
[32] D. Hooper, P. Blasi, and P. D. Serpico, J. Cosmol. Astropart. Phys. 01 (**2009**) 025; H. Yuksel, M. D. Kistler, and T. Stanev, Phys. Rev. Lett. **103**, 051101 (2009); S. Profumo, Central Eur. J. Phys. **10**, 1 (2012).
[33] M. Blennow, J. Edsjo, and T. Ohlsson, J. Cosmol. Astropart. Phys. 01 (**2008**) 021.
[34] G. L. Fogli, E. Lisi, A. Marrone, D. Montanino, A. Palazzo, and A. M. Rotunno, Phys. Rev. D **86**, 013012 (2012).
[35] M. Nauenberg, Phys. Rev. D **36**, 1080 (1987).
[36] K. Griest and D. Seckel, Nucl. Phys. **B283**, 681 (1987); Nucl. Phys. **B296**, 1034(E) (1988).
[37] V. Berezinsky, A. Bottino, J. R. Ellis, N. Fornengo, G. Mignola, and S. Scopel, Astropart. Phys. **5**, 333 (1996).
[38] G. Jungman, M. Kamionkowski, and K. Griest, Phys. Rep. **267**, 195 (1996).
[39] M. Cirelli, N. Fornengo, T. Montaruli, I. A. Sokalski, A. Strumia, and F. Vissani, Nucl. Phys. **B727**, 99 (2005); Nucl. Phys. **B790**, 338(E) (2008).
[40] P. Gondolo, J. Edsjo, P. Ullio, L. Bergstrom, M. Schelke, and E. A. Baltz, J. Cosmol. Astropart. Phys. 07 (**2004**) 008.
[41] R. Abbasi *et al.* (IceCube Collaboration), Astropart. Phys. **35**, 615 (2012).
[42] J. F. Beacom and J. Candia, J. Cosmol. Astropart. Phys. 11 (**2004**) 009.
[43] R. Gandhi, C. Quigg, M. H. Reno, and I. Sarcevic, Phys. Rev. D **58**, 093009 (1998).
[44] T. Sjostrand, S. Mrenna, and P. Z. Skands, J. High Energy Phys. 05 (**2006**) 026.
[45] M. G. Aartsen *et al.* (IceCube Collaboration), Phys. Rev. Lett. **110**, 151105 (2013).
[46] M. Honda, T. Kajita, K. Kasahara, S. Midorikawa, and T. Sanuki, Phys. Rev. D **75**, 043006 (2007).
[47] S. Andreas, M. H. G. Tytgat, and Q. Swillens, J. Cosmol. Astropart. Phys. 04 (**2009**) 004.
[48] A. Bottino, F. Donato, N. Fornengo, and S. Scopel, Phys. Rev. D **70**, 015005 (2004).
[49] V. Niro, A. Bottino, N. Fornengo, and S. Scopel, Phys. Rev. D **80**, 095019 (2009).
[50] T. Bruch, A. H. G. Peter, J. Read, L. Baudis, and G. Lake, Phys. Lett. B **674**, 250 (2009).
[51] J. Leute, A. Groß and, E. Resconi, Proceedings of the 33rd ICRC, Rio de Janeiro 2013 (to be published).
[52] E. Middell, J. McCartin, and M. D'Agostino, Proceedings of the 31st ICRC, Lodz 2009 (to be published).
[53] J. Kumar, J. G. Learned, M. Sakai, and S. Smith, Phys. Rev. D **84**, 036007 (2011).
[54] J. G. Learned, arXiv:0902.4009.
[55] J. Peltoniemi, arXiv:0909.4974.
[56] M. Lindner, A. Merle, and V. Niro, Phys. Rev. D **82**, 123529 (2010).
[57] R. Allahverdi, S. Bornhauser, B. Dutta, and K. Richardson-McDaniel, Phys. Rev. D **80**, 055026 (2009).
[58] A. Falkowski, J. Juknevich, and J. Shelton, arXiv:0908.1790.
[59] D. J. Koskinen, Mod. Phys. Lett. A **26**, 2899 (2011).
[60] R. Auer, Nucl. Instrum. Methods Phys. Res., Sect. A **602**, 84 (2009).
[61] M. G. Aartsen *et al.* (IceCube Collaboration), Phys. Rev. Lett. **110**, 131302 (2013).
[62] H. Yuksel, S. Horiuchi, J. F. Beacom, and S. 'i. Ando, Phys. Rev. D **76**, 123506 (2007).
[63] K. Daum *et al.* (Frejus. Collaboration), Z. Phys. C **66**, 417 (1995); J. Ahrens *et al.* (AMANDA Collaboration), Phys. Rev. D **66**, 012005 (2002); Y. Ashie *et al.* (Super-Kamiokande Collaboration), *ibid.* **71**, 112005 (2005).